DEUTSCHES ELEKTRONEN-SYNCHROTRON DESY

DESY 80/120
December 1980

HIGHER ORDER QCD CORRECTIONS IN e^+e^- ANNIHILATION INTO HADRONS

by

G. Schierholz
II. Institut für Theoretische Physik der Universität Hamburg

NOTKESTRASSE 85 · 2 HAMBURG 52

To be sure that your preprints are promptly included in the
HIGH ENERGY PHYSICS INDEX ,
send them to the following address (if possible by air mail) :

DESY
Bibliothek
Notkestrasse 85
2 Hamburg 52
Germany

DESY 80/120
December 1980

Higher Order QCD Corrections in e^+e^- Annihilation into Hadrons

by

G. Schierholz

II. Institut für Theoretische Physik der Universität Hamburg

Invited talk given at the ≫ Symposium on Topical Questions in QCD, Niels Bohr Institute, Copenhagen, 9 - 13 June 1980 ≪ and ≫ International Summer Institute on Theoretical Physics, Bad Honnef, 1 - 12 September 1980 ≪

1. Introduction

Quantum chromodynamics (QCD) has permeated almost all fields of strong interaction physics and needs no further introduction. Experimentally, there are various qualitative and even semi-quantitative pieces of evidence in favour of QCD. But so far there is no convincing proof of its validity. Though it has no real competition, I feel it is extremely important to think out tests which emphasize the more fundamental and discriminative aspects of QCD as, e.g., its nonabelian gauge structure. Such tests are rare and not easy to perform as we shall see.

Electron-positron annihilation into hadrons is particularly suited for this task. For example, it is essentially background-free, and the presently available energies allow to probe distances smaller than 10^{-15} cm. It is not by accident that the strongest evidence for the existence of gluons follows from the observation of three-jet events at PETRA [1].

It is obvious that observables which are sensitive to the distinctive elements of the theory will involve higher-order contributions as QCD shows its full gauge structure only in order α_s^2. But also for a quantitative analysis, i.e., a meaningful determination of α_s and Λ, it will be necessary to include order α_s^2 corrections. The point of wanting to know Λ precisely is that it can, e.g., be calculated in lattice QCD using strong coupling expansions. The recent calculation of Münster and Weisz [2] suggests $\Lambda_{lattice} \approx 1.7$ MeV which, in the continuum theory, corresponds to [3,4] ($N_f = 0$)

$$\Lambda_{\overline{MS}} \approx 48 \text{ MeV}. \qquad (1.1)$$

It would be a great support for QCD if that, or something near that, came out experimentally.

In this talk I shall discuss the phenomenological profile of order α_s^2 corrections to e^+e^- annihilation into hadrons. In order to get an idea of how sensitive the predictions are to, e.g., the nonabelian gluon self-couplings, I shall, at given times, also comment on the would-be results of the abelian vector theory.

In Section 2 I shall make a few comments about the total cross section $\sigma(e^+e^- \rightarrow \text{hadrons})$. In Section 3 I shall mention some new results on event shapes of four-jet final states. Section 4 introduces an intriguing possibility to "directly" measure the colour charge of gluons. In Section 5 I shall discuss three-jet inclusive cross sections. Section 6, finally, contains a brief summary.

2. The Total Cross Section

One of the first quantities being studied in this context is the total hadronic cross section. The order α_s^2 corrections have been calculated by various authors [5]. In the $\overline{\text{MS}}$ renormalization scheme [6] it gives

$$\sigma = \sigma_0 \left[1 + \frac{\alpha_s(Q^2)}{\pi} + \left(\frac{\alpha_s(Q^2)}{\pi} \right)^2 (1.986 - 0.115 N_f) \right] , \qquad (2.1)$$

where

$$\alpha_s(Q^2) = \frac{4\pi}{\beta_0 \ln Q^2/\Lambda^2 + \beta_1/\beta_0 \ln(\ln Q^2/\Lambda^2)} ,$$

$$\beta_0 = 11 - \tfrac{2}{3} N_f \quad , \quad \beta_1 = 102 - \tfrac{38}{3} N_f , \qquad (2.2)$$

N_f being the number of flavours, and σ_0 is the Born cross section.

Like any other finite order result this is renormalization prescription dependent. That is to say, if σ (Eq. (2.1)) is calculated in two different renormalization schemes it will generally differ by a term $O(\alpha_s^3)$. The question of rapid convergence of the perturbation series is then largely a question of the renormalization scheme (at least for the total cross section). For example, the order α_s^2 correction to σ can be totally absorbed into the nontrivial lowest order contribution, i.e.,

$$\sigma = \sigma_0 \left[1 + \frac{\alpha_s(Q^2)}{\pi} \right] \qquad (2.3)$$

($O(\alpha_s^3)$ terms neglected), by the change of scale parameters (TS total subtraction scheme)

$$\Lambda_{\overline{\text{MS}}} \rightarrow \Lambda_{\text{TS}} = e^{\frac{4}{\beta_0}(1.986 - 0.115 N_f)} \Lambda_{\overline{\text{MS}}}$$

$$= 1.44 \, \Lambda_{\overline{\text{MS}}} \qquad (2.4)$$

$$N_f = 5$$

The problem of how to minimize higher uncalculated orders of perturbation theory has been addressed to by Stevenson in a recent paper [7]. The "optimum" result differs only imperceptibly from the total cross section calculated in the TS and $\overline{\text{MS}}$ scheme. In the $\overline{\text{MS}}$ scheme higher order corrections appear to converge reasonably well also in a variety of other processes [8].

The main result of this calculation is that higher order corrections to the total cross section are small. Experimentally, these have, however, little

significance as it would mean to measure the total cross section with unprecedented accuracy. Mind you, the present experimental error (statistical and systematic) has the same magnitude as the first order contribution (and this is unlikely to change in the near future), while the order α_s^2 corrections give rise to a $\lesssim 0.5$ % effect on the zeroth order background.

As we shall see, one stands a better chance to see effects of higher order contributions on a $O(\alpha_s)$ background, that is in multi-jet final states.

3. Four-Jet Final States

Four-jet final states (Fig. 1) are most favourable in this respect. With increasing energy we expect that they can easily be separated experimentally. In fact, evidence for four-jet events has recently been reported by various groups at PETRA, and we hope that sufficiently high statistics will be accumulating in the next few years.

The rates for four-jet production have been calculated and discussed in Ref. 9. The only remark I like to add to this topic is that other methods of extracting four-jet events might be more favourable (as far as the rates go) than employing an acoplanarity cut-off. I am thinking here, e.g., of a mass cut-off or a cluster analysis [10].

In this section of my talk I shall rather focus on a more unambiguous test of QCD. That is, I will be discussing angular correlations within the four-jet events which are more directly related to the triple-gluon coupling.

Let us consider those four-jet events which consist of two back-to-back jets as shown in Fig. 2 (in contrast to events with one jet in one hemisphere and three in the other). They can be marked off by the following procedure: first determine the thrust axis of each event and then demand that the invariant mass squared in both hemispheres (L left, R right) is larger than a given M^2, i.e.,

$$\left(\sum_{i\in L,R} E_i\right)^2 - \left(\sum_{i\in L,R} p_{i\parallel}\right)^2 = \left(\sum_{i\in L,R} E_i\right)^2 - T^2\frac{Q^2}{4} = M_{L,R}^2 \geq M^2 \qquad (3.1)$$

(T thrust). We shall employ a rather large cut-off mass,

$$M = 0.2\,Q\,, \qquad (3.2)$$

which will effectively remove the background from two- and three-jet events, and which will keep the soft and collinear singularities at $M = 0$ at a distance in order for a perturbative calculation to be credible. The above cut-off leads to the production rate

$$\sigma^{4\text{-jet}}(M)/\sigma_0 \approx 2\,\% \qquad (3.3)$$

for $\frac{\alpha_s}{\pi} = 0.05$ which corresponds to $\Lambda = 0.3$ GeV at $Q = 30$ GeV and $N_f = 5$ or $\Lambda = 0.4$ GeV at $Q = 40$ GeV.

In order to underline the effect of the triple-gluon coupling contribution we shall compare the QCD results to a vector theory with colour-triplet quarks

(which are needed to be in agreement with the measured total cross section) and colour-singlet gluons. This we shall refer to as "QED". The quark-gluon coupling constant will be fixed as to give the same three-jet production cross section, i.e.,

$$\alpha_{\text{"QED"}} = \frac{4}{3}\,\alpha_s \quad . \tag{3.4}$$

The two-jet planes in opposite hemispheres define an azimuthal angle ϕ between the normals of the two planes as indicated in Fig. 2. The normals can be oriented by, e.g., identification of quark and gluon jets. That is

$$\vec{n}_L = \vec{p}_q \times \vec{p}_g \quad , \quad \vec{n}_R = \vec{p}_{\bar{q}} \times \vec{p}_g \quad . \tag{3.5}$$

Let me argue now what we expect the ϕ -distributions to look like for QCD and "QED". For the sake of argument it is sufficient to consider only the leading contribution from two back-to-back qg and $\bar{q}g$ jets. In "QED" the dominant diagram is that shown in Fig. 3a which, at the leading log level, does not give rise to any azimuthal correlation. This is to say, that here the ϕ -distribution should be similar to the phase-space distribution, given that subleading contributions can be neglected. The phase-space distribution is plotted in Fig. 4 for the mass cut-off (3.2). The decrease near $\phi = 0^\circ$ is due to the fact that all four-jet events with $M_{L,R} \geq \frac{1}{4}\sqrt{2}$ are necessarily nonplanar. In QCD, on the other hand, we expect a strong (dynamical) azimuthal correlation arising from the interference of diagrams

(a) and (b) shown in Fig. 3. The dominant contribution comes from the region where both the angles between the quark/antiquark and gluon jets and the two gluon jets are small due to the collinear gluon singularities. As a result, the two jet planes will be predominantly parallel.

Now to the actual calculations [11]. Let us first consider the case of non-oriented normals (being symmetric with respect to $\vec{n} \to -\vec{n}$) which leads to a symmetric ϕ -distribution under $\phi \to \pi - \phi$. Figure 5 shows $\frac{1}{\sigma_0}\frac{d\sigma}{d\phi}$ for QCD and "QED". As expected, we find that the two planes have a strong tendency to be parallel in QCD, while in "QED" the two planes tend to be orthogonal in very good agreement with the phase space distribution (Fig. 4).

In QCD we found that $\approx$ 80 % of the events considered here have a quark plus a gluon in one hemisphere and an antiquark plus a gluon in the other. If one day we will be able to separate between quark and gluon jets, we should find those planar events to dominate which have the two gluon jets on the same side of the thrust axis. This, again, is suggested by the gluon self-coupling diagram shown in Fig. 3b.

For this dominant subsample we introduce an oriented normal according to (3.5). The outcoming ϕ -distribution is shown in Fig. 6. It is seen that the configuration where the two gluon jets are "closest" is indeed favoured.

4. Probing Virtual Corrections: Forward-Backward Asymmetry

Observables which only involve three-jet final states but still are sensitive to the self-interaction of gluons are a little harder to construct as they will encounter loops. On the other hand, three-jet events are a lot easier

to separate given the limited energies of PETRA and PEP.

There are essentially two classes of observables which are of interest here. The interference cross sections that are associated with the imaginary part of the loop-corrected three-jet diagrams (Fig. 7) form one class. The other class includes the Sterman-Weinberg [12] type three-jet cross sections. In this section I shall concentrate on the first class and leave the second class for later discussion.

In second order perturbation theory the imaginary part of the hadronic tensor $H_{\mu\nu}$, given by the diagrams in Fig. 7, is infrared finite by itself. With p_1, p_2 and p_3 being the quark, antiquark and gluon momenta, respectively, it can be written *) ($x_i = 2E_i/Q$, $x_1+x_2+x_3 = 2$)

$$\mathrm{Im}\, H_{ij} = (p_{1i}p_{2j} - p_{2i}p_{1j})\, C(x_1,x_2) \quad , \quad i,j = 1,2,3 \, , \tag{4.1}$$

or equivalently,

$$\mathrm{Im}\, \vec{H} = \vec{p}_1 \times \vec{p}_2 \; C(x_1,x_2) \quad , \quad \vec{H} = (H_{23}, H_{31}, H_{12}) , \tag{4.2}$$

thus corresponding to a (normal) vector perpendicular to the event plane. In order to turn the imaginary part into an observable one, accordingly, will need another vector to multiply $\mathrm{Im}\,\vec{H}$. Conceivable are the (longitudinal) electron/positron beam polarization vector, the electron/positron momentum vector and the (transversal) polarization vector of the outgoing quark and antiquark,

*) Note that the time components of the hadronic tensor are zero due to current conservation.

respectively. The latter would require to measure the polarization of the quark or antiquark. Note that $\mathrm{Im}\, H_{ij}$ vanishes in the two-jet limit.

Let us first consider massless quarks. It is well known that the (complete) hadronic tensor H_{ij} is infrared singular. After dimensional regularization these singularities appear as poles $1/(n-4)^2$ and $1/(n-4)$. The reason I mention this here is that the antisymmetric part of the residue of the single pole term, $\mathrm{Res}\, H_{[ij]}$, is related to $\mathrm{Im}\, H_{ij}$ by

$$\mathrm{Im}\, H_{ij} = -\frac{\pi}{2}\, \mathrm{Res}\, H_{[ij]} \, , \tag{4.3}$$

which has some interesting consequences.

The infrared singularities of the loop-corrected three-jet diagrams are supposed to cancel against those of the four-jet diagrams (Fig. 1) when combined to properly defined jet cross sections, which are insensitive to the emission of soft and/or collinear quanta. Since the hadronic tensor associated with four jets is symmetric, we conclude that $\mathrm{Im}\, H_{ij} = 0$ for massless quarks *). This is to say that, to order α_s^2, there is no observable final state interaction effect. It would be interesting to find out whether this result holds also in higher orders. Exactly the same arguments go through for orthoquarkonium decay into gluons, i.e.,

*) We have also calculated H_{ij} term by term which gave the same result [13].

$$e^+e^- \to Q\bar{Q} \to ggg \ , \tag{4.4}$$

and I would expect Im $H_{ij} = 0$ here as well *).

For massive quarks Eq. (4.3) is no longer valid and Im $H_{ij} \neq 0$ generally. Let me discuss this case now. Due to lack of time I shall restrict myself to considering only the first two of the observables indicated after Eq. (4.3), in which the sum over the quark/antiquark polarizations is taken. In this event the cross section measuring Im $\vec{H}$ is given by (apart from kinematical factors)

$$\mathrm{Im}\, L_{ij} \cdot \mathrm{Im}\, H_{ij} = \mathrm{Im}\,\vec{L} \cdot \mathrm{Im}\,\vec{H} \ , \quad \vec{L} = (L_{23}, L_{31}, L_{12}) \ , \tag{4.5}$$

where L_{ij} is the leptonic tensor. For Im $\vec{L}$ to be nonzero we need <u>either</u> longitudinally polarized electron and/or positron beams, which yields [15]

$$\mathrm{Im}\,\vec{L} = -\vec{S} = L\vec{e}^{\,(-)} \ , \quad L = h^{(+)} - h^{(-)} \ , \tag{4.6}$$

where $\vec{e}^{\,(-)}$ is the unit vector in the direction of the electron beam and $h^{(+)}$ the electron/positron helicity, <u>or</u> the presence of weak and electromagnetic interferences, which yields [16]

$$\mathrm{Im}\,\vec{L} = (-4 Q_f v_f \,\mathrm{Re}\,\chi + 4 v (1+v_f^2) |\chi|^2)\, \vec{p}^{\,(-)}/Q \ , \tag{4.7}$$

*) De Rujula, Petronzio and Lautrup [14], though, obtain a small, but finite, result.

where $\vec{p}^{\,(-)}$ is the electron beam momentum and

$$v = -1 + 4\sin^2\theta_W \ , \quad v_f = \begin{cases} 1 - \frac{8}{3}\sin^2\theta_W & Q_f = \frac{2}{3} \\ -1 + \frac{4}{3}\sin^2\theta_W & Q_f = -\frac{1}{3} \end{cases} \tag{4.8}$$

$$\chi = 4.49 \cdot 10^{-5}\,\mathrm{GeV}^{-2} M_Z^2 \ \frac{Q^2}{Q^2 - M_Z^2 + i M_Z \Gamma_Z} \ .$$

As can readily be seen Im $\vec{L}$ · Im $\vec{H}$ is T-odd in the first case, while it is T- and P-odd in the second. Transverse beam polarization does not contribute to Im $\vec{L}$.

Physically, Im $\vec{L}$ · Im $\vec{H}$ will give rise to a forward-backward asymmetry of the normal to the event plane, as should be clear now. Let us therefore introduce the asymmetry

$$A = \frac{\dfrac{d^3\sigma(\cos\Theta = |\cos\Theta|)}{d\cos\Theta\, dx_1 dx_2} - \dfrac{d^3\sigma(\cos\Theta = -|\cos\Theta|)}{d\cos\Theta\, dx_1 dx_2}}{\dfrac{d^3\sigma(\cos\Theta = |\cos\Theta|)}{d\cos\Theta\, dx_1 dx_2} + \dfrac{d^3\sigma(\cos\Theta = -|\cos\Theta|)}{d\cos\Theta\, dx_1 dx_2}} \ , \tag{4.9}$$

where Θ is the angle between the normal of the event plane, defined here as $\vec{n} = \mathrm{sign}(x_1 - x_2)\, \vec{p}_1 \times \vec{p}_2$, and the electron beam direction. For A we then obtain

$$A \approx 2P \frac{\cos\Theta}{1+\frac{1}{2}\sin^2\Theta} H_{12} \left[\frac{d^2\sigma}{dx_1 dx_2}\right]$$

$$\equiv 2P \frac{\cos\Theta}{1+\frac{1}{2}\sin^2\Theta} R \qquad (4.10)$$

$$P = \begin{cases} (h^{(-)} - h^{(+)}) / (1 - h^{(-)}h^{(+)}) \\ \dfrac{-2Q_f v_f \mathrm{Re}\chi + 2v(1+v_f^2)|\chi|^2}{Q_f^2 - 2Q_f v v_f \mathrm{Re}\chi + (1+v^2)(1+v_f^2)|\chi|^2} \end{cases} \qquad (4.11)$$

The parameter P corresponding to γ-Z interference has been drawn in Fig. 8. It is found to be quite large already at the upper PETRA energies.

The ratio R has been calculated [17] for quark mass ratios $m_q/Q = 0.125$ and $m_q/Q = 0.25$. The result is shown in Fig. 9 (same α_s as before) for various thrust values as a function of the angle between the quark and antiquark jet. The asymmetry depends quite strongly on the value of m_q/Q. In favourable cases we may expect an asymmetry of more than ten per cent which is very encouraging. For the bottom quark ($m \approx 5$ GeV) and $Q = 40$ GeV, where we find already a substantial admixture of the weak neutral current ($P \approx 0.3$), the effect will be still on the per cent level.

Why now is it worth bothering about the asymmetry A which is not exactly easy to measure? The answer is that R "directly" measures the colour charge of the gluons.

According to the two classes of diagrams contributing to Im H_{ij}, those involving the triple-gluon coupling and the "QED" diagrams, R can be written

$$R = \frac{1}{N} \mathrm{Tr}\left(i f_{\alpha\beta\gamma} \frac{\lambda_\beta}{2} \frac{\lambda_\gamma}{2} \frac{\lambda_\alpha}{2}\right) r_C + \frac{1}{N} \mathrm{Tr}\left(\frac{\lambda_\beta}{2} \frac{\lambda_\alpha}{2} \frac{\lambda_\beta}{2} \frac{\lambda_\alpha}{2}\right) r_E \,, \qquad (4.12)$$

where $r_C \approx r_E$. Noticing that $\frac{1}{N} \mathrm{Tr}\left(i f_{\alpha\beta\gamma} \frac{\lambda_\beta}{2} \frac{\lambda_\gamma}{2} \frac{\lambda_\alpha}{2}\right) = -2$ and $\frac{1}{N} \mathrm{Tr}\left(\frac{\lambda_\beta}{2} \frac{\lambda_\alpha}{2} \frac{\lambda_\beta}{2} \frac{\lambda_\alpha}{2}\right) = -\frac{2}{9}$, this gives ($\alpha_s$ "QED" $= \frac{4}{3}\alpha_s$)

$$R_{\text{"QED"}} \approx -\frac{4}{5} R_{QCD} \,. \qquad (4.13)$$

In order to prove (or disprove) QCD it would be sufficient to establish the sign of R.

The asymmetry A can also be looked at as a clean and precise measure of the heavy quark masses as it critically depends on m_q/Q.

5. Three-Jet (Inclusive) Cross Sections

As has been mentioned already, the loop-corrected three-jet diagrams (Fig. 7, self-energy diagrams not shown) are infrared singular and so are the four-jet diagrams (Fig. 1) in the three-jet limit. The question if these infrared (and collinear) singularities cancel in suitably defined cross sections, and what these cross sections are, has received great interest over the last few years. Here we shall discuss two species of cross sections which turn out to be infrared finite, the Sterman-Weinberg [12] type three-jet cross section and $d\sigma/dT$ (T thrust).

We perform renormalization in the $\overline{\text{MS}}$ scheme [6] which corresponds to the subtraction of the ultra-violet poles and the associated factors of $(\ln 4\pi - \delta)$. The cross section for three-jet events which have all but a fraction 2ϵ of the total energy distributed within three separated cones of (full) opening angle δ is given by [18]

$$\frac{1}{\sigma}\frac{d^2\sigma^{3\text{-jet}}(\epsilon,\delta)}{dx_1\,dx_2} = \frac{2}{3}\frac{\alpha_s(Q^2)}{\pi}\frac{\sigma_0}{\sigma}\left[\frac{x_1^2+x_2^2}{(1-x_1)(1-x_2)}\left\{1-\frac{\alpha_s(Q^2)}{\pi}\left[\left(\frac{4}{3}\ln\frac{\epsilon}{x_1}+\frac{4}{3}\ln\frac{\epsilon}{x_2}\right.\right.\right.\right.$$

$$+3\ln\frac{\epsilon}{x_3}+\frac{19}{4}-\frac{N_f}{6}\Big)\ln\frac{1-\cos\delta}{2}-\ln\epsilon\left(3\ln\frac{1-\cos\theta_{13}}{2}+3\ln\frac{1-\cos\theta_{23}}{2}\right.$$

$$\left.-\frac{1}{3}\ln\frac{1-\cos\theta_{12}}{2}\right)-\left(\frac{4}{3}\frac{\epsilon}{x_1}+\frac{4}{3}\frac{\epsilon}{x_2}+3\frac{\epsilon}{x_3}\right)\ln\frac{1-\cos\delta}{2}+\left(\frac{11}{2}-\frac{N_f}{3}\right)\ln x_3$$

$$\left.\left.\left.+R(x_1,x_2)\right]\right\}+\frac{\alpha_s(Q^2)}{\pi}F(x_1,x_2)\right]+O(\epsilon)+O(\delta^2)\,, \tag{5.1}$$

where

$$R(x_1,x_2) = \Big[\ln x_3\left(3\ln\frac{1-x_3}{x_3}-\frac{3}{2}\ln x_1\right)-\frac{1}{6}\ln(1-x_3)(\ln x_1+\ln(1-x_1))$$

$$-\ln x_1\left(2\ln x_1+\frac{4}{3}\ln(1-x_1)-\frac{3}{2}\ln(1-x_2)+2\right)+\frac{3}{2}\mathcal{X}_2\left(\frac{1-\cos\theta_{13}}{2}\right)-\frac{4}{3}\mathcal{X}_2(1-x_1)$$

$$+(x_1\longleftrightarrow x_2)\Big]+\frac{3}{2}\ln\frac{1-x_1}{x_3}\ln\frac{1-x_2}{x_3}+\frac{1}{3}\ln x_3\ln(1-x_3)+\frac{1}{6}\ln x_1\ln x_2$$

$$-\frac{1}{6}\mathcal{X}_2\left(\frac{1-\cos\theta_{12}}{2}\right)+\frac{1}{3}\mathcal{X}_2(1-x_3)+\frac{13}{18}N_f+\frac{2}{3}\pi^2-\frac{44}{3}\,, \tag{5.2}$$

$$F(x_1,x_2) = \frac{x_3^2}{(1-x_1)(1-x_2)}\left\{\frac{1}{12}\Big[\ln(1-x_3)\ln(1-x_1)-\ln x_1\ln(1-x_1)-\mathcal{X}_2(1-x_1)+(x_1\longleftrightarrow x_2)\Big]\right.$$

$$-\frac{1}{6}\ln x_3\ln(1-x_3)-\frac{1}{6}\mathcal{X}_2(1-x_3)+\frac{N_f}{12}+\frac{\pi^2}{36}-\frac{11}{12}\Big\}+\frac{x_3}{(1-x_1)(1-x_2)}\left\{\frac{1}{6}\Big[-\ln(1-x_3)\ln(1-x_1)\right.$$

$$+\ln x_1\ln(1-x_1)+\mathcal{X}_2(1-x_1)+(x_1\longleftrightarrow x_2)\Big]+\frac{1}{3}\ln x_3\ln(1-x_3)+\frac{1}{3}\mathcal{X}_2(1-x_3)$$

$$\left.-\frac{\pi^2}{18}+\frac{5}{6}\right\}+\frac{1}{6}\Big[\ln(1-x_3)\ln(1-x_1)-\ln x_1\ln(1-x_1)+16\ln(1-x_1)$$

$$-\mathcal{X}_2(1-x_1)+(x_1\longleftrightarrow x_2)\Big]-\frac{1}{3}\ln x_3\ln(1-x_3)-\frac{1}{3}\mathcal{X}_2(1-x_3)+\frac{\pi^2}{18}+\frac{1}{6}$$

$$+\frac{1}{12}\left[\frac{x_1^2-x_2^2}{(1-x_1)(1-x_2)}\left(\ln(1-x_3)\ln(1-x_1)-\ln x_1\ln(1-x_1)-\mathcal{X}_2(1-x_1)\right)+(x_1\longleftrightarrow x_2)\right]$$

$$-\frac{2}{3}\left[\frac{1-x_1}{x_1}+\left(4(1-x_2)-\frac{17}{4}(1-x_1)\right)\frac{\ln(1-x_1)}{x_1}+(1-x_1)(1-x_2)\frac{\ln(1-x_1)}{x_1^2}+(x_1\longleftrightarrow x_2)\right]$$

$$-\frac{1}{3}\frac{1-x_3}{x_3}\left(1+\frac{1+x_3}{x_3}\ln(1-x_3)\right)\,, \tag{5.3}$$

$$\mathcal{X}_2(x) = -\int_0^x dz\;\frac{\ln(1-z)}{z}\,. \tag{5.4}$$

The cosines of the angles between the jet axes can be expressed in terms of the (scaled) energies of the quark (x_1), antiquark (x_2) and gluon jet (x_3) by

$$\cos\Theta_{ij} = 1 - \frac{2}{x_i x_j}\,(x_i + x_j - 1)\,. \tag{5.5}$$

The $O(\epsilon)$, $O(\delta^2)$ terms are too lengthy to write down and are calculated numerically. As can readily be checked, the (dominant) $\ln\epsilon$, $\ln\delta$ terms in (5.1) agree with an earlier leading logarithm calculation of Smilga and Vysotsky *) 19).

The cross section (5.1) has been plotted versus thrust for two choices of ϵ, δ in Fig. 10 (same α_s as before). With decreasing ϵ, δ it decreases rapidly and becomes increasingly steeper than the Born cross section (for $\epsilon \lesssim 2(1-T)$ and $(1-\cos\delta)/2 \lesssim 2(1-T)$). The latter is mainly due to the term (cf. Eq. (5.1))

$$-\frac{2}{3}\left(\frac{\alpha_s(Q^2)}{\pi}\right)^2 \frac{\sigma_0}{\sigma}\,\frac{x_1^2+x_2^2}{(1-x_1)(1-x_2)}\left(\frac{11}{2}-\frac{N_f}{3}\right)\ln x_3\,, \tag{5.6}$$

while the remaining logarithms and Spence functions in $R(x_1,x_2)$ and $F(x_1,x_2)$ are finite in the limit $x_1, x_2 \to 1$ or cancel against $-3\ln x_3 \ln\frac{1-\cos\delta}{2}$ (note that the angles between the jets must not be smaller than δ).

The expression (5.6) can be absorbed into the strong coupling constant by the change of scales

*) Note the difference in notation and that Ref. 19 contains a misprint.

$$Q^2 \to x_3^2 Q^2\,, \quad \alpha_s(Q^2) \to \alpha_s(x_3^2 Q^2)\,. \tag{5.7}$$

In other words, if the three-point vertex is renormalized at $x_3^2Q^2$ rather than Q^2 the loop corrections give rise to logarithms which exactly cancel (5.6). This is quite conceivable as in the two-jet limit the four-momentum squared, which determines the strength of the quark-gluon coupling, becomes much smaller than Q^2 which only provides the natural scale when all jet angles are large.

The thrust distribution $\frac{1}{\sigma}\frac{d\sigma}{dT}$ will also involve the four-jet cross section. We can write

$$\frac{1}{\sigma}\frac{d\sigma}{dT} = \frac{1}{\sigma}\frac{d\sigma^{3\text{-jet}}(\epsilon,\delta)}{dT} + \frac{1}{\sigma}\frac{d\sigma^{4\text{-jet}}(\epsilon,\delta)}{dT}\,, \tag{5.8}$$

where $d\sigma^{4\text{-jet}}(\epsilon,\delta)$ is the proper four-jet cross section with jet energies larger than $\frac{\epsilon}{2}Q$ and relative jet angles larger than δ. Clearly, (5.8) is independent of the particular choice of ϵ, δ.

In Fig. 11 I have drawn $\frac{1}{\sigma}\frac{d\sigma}{dT}$ for the $\overline{\text{MS}}$ and TS renormalization scheme. The shape of the thrust distribution is visibly different from the Born distribution. The enhancement at lower thrust values is entirely due to four-jet production. At larger thrust values the three-jet cross section takes over which gives a negative correction and, eventually, will make $\frac{1}{\sigma}\frac{d\sigma}{dT}$ negative at very large T (not drawn anymore). This is exactly what we expect from the leading logarithm formula 20)

$$\frac{1}{\sigma}\frac{d\sigma}{dT} \underset{T\to 1}{\simeq} -\frac{32}{9}\left(\frac{\alpha_s(Q^2)}{\pi}\right)^2 \frac{|\ln(1-T)|^3}{1-T} \qquad (5.9)$$

(which can also be read off from (5.1) noticing that $\epsilon \lesssim 2(1-T)$ and $(1-\cos\delta)/2 \lesssim 2(1-T)$).

It is quite instructive now to absorb the order α_s^2 corrections into the Born cross section (similar to (2.4), allowing for a thrust dependent α_s) and re-express them in terms of an effective scale parameter Λ. Obviously, this is only possible for $T \gtrsim 2/3$ but not in the region $1/\sqrt{3} \leq T \leq 2/3$ which is only populated by four-jet events. As a result Λ_{eff} will go to infinity as $T \to 2/3$. The effective Λ is shown in Fig. 12. It indicates that Λ will change substantially if higher-order corrections are included. For example, the fit to the lowest order distribution would give $\Lambda \approx 0.05$ GeV at higher T and $\Lambda \approx 0.5$ GeV at lower T instead of an universal $\Lambda_{\overline{\text{MS}}} = 0.3$ GeV. If, experimentally, the effective Λ turned out to have the predicted form (Fig. 12), I feel this would be a great triumph for perturbative QCD.

We conclude that in the $\overline{\text{MS}}$ (and TS) scheme the perturbation series for $d\sigma/dT$ is well behaved (as one might have expected from the total cross section), perhaps excluding the very large thrust region. On the other hand, the effects of higher orders are large enough to be detected.

It should be said that a similar investigation to this section has been performed by Ellis, Ross and Terrano [21] who found a much larger order α_s^2 correction.

6. Summary

At present and for some time to come, PETRA and PEP are the most powerful "microscopes" for probing the short-distance structure of hadrons, and we hold out greatest hopes that these two machines will serve to establish (or disprove) QCD.

As we have seen, QCD makes quite a few unambiguous predictions for e^+e^- annihilation into hadrons. It lies in the nature of perturbative QCD that the measurable effects of the distinctive elements of the theory are only of the order of a few times α_s^2. But with higher statistics accumulating in the next few years it should be possible to perform the proposed tests successfully.

Asked what prediction I think has the best prospect of being tested in the nearest future, I would say the azimuthal correlation of the two back-to-back jet planes.

Acknowledgement

I would like to thank my various co-workers on the subject of this talk for a prolific collaboration.

References

1) R. Brandelik et al., Phys. Letters 86B, 243 (1979);
D.P. Barber et al., Phys. Rev. Letters 43, 830 (1979);
Ch. Berger et al., Phys. Letters 86B, 418 (1979);
W. Bartel et al., Phys. Letters 91B, 142 (1979).

2) G. Münster and P. Weisz, DESY preprint DESY 80/57 (1980).

3) A. and P. Hasenfratz, CERN preprint CERN-TH 2827 (1980).

4) W. Celmaster and R.J. Gonsalves, Phys. Rev. D20, 1420 (1979).

5) M. Dine and J. Sapirstein, Phys. Rev. Letters 43, 668 (1979);
W. Celmaster and R.J. Gonsalves, UCSD preprint UCSD-10P10-206, 207 (1979);
K.G. Chetyrkin, A.L. Kataev and F.V. Tkachov, Phys. Letters 85B, 277 (1979).

6) W.A. Bardeen, A.J. Buras, D.W. Duke and T. Muta, Phys. Rev. D18, 3998 (1978).

7) P.M. Stevenson, Madison preprint DOE-ER/0881-153 (1980).

8) C.H. Llewellyn-Smith, talk given at the XXth International Conference on High Energy Physics, University of Wisconsin, Madison; 1980.

9) A. Ali, J.G. Körner, Z. Kunszt, J. Willrodt, G. Kramer, G. Schierholz and E. Pietarinen, Phys. Letters 82B, 285 (1979) and Nucl. Phys. B167, 454 (1980); K.J.F. Gaemers and J.A.M. Vermaseren, CERN preprint CERN-TH 2816 (1980).

10) Ch. Berger et al., DESY preprint DESY 80/93 (1980).

11) J.G. Körner, G. Schierholz and J. Willrodt, DESY preprint DESY 80/119 (1980).

12) G. Sterman and S. Weinberg, Phys. Rev. Letters 39, 1436 (1977).

13) J.G. Körner, G. Kramer, G. Schierholz, K. Fabricius and I. Schmitt, Phys. Letters 94B, 207 (1980).

14) A. De Rujula, R. Petronzio and B. Lautrup, Nucl. Phys. B146, 50 (1978).

15) E.g., N.M. Avram and D.H. Schiller, Nucl. Phys. B70, 272 (1974).

16) G. Schierholz and D.H. Schiller, DESY preprint DESY 80/88 (1980).

17) K. Fabricius, I. Schmitt, G. Kramer and G. Schierholz, DESY preprint DESY 80/17 (1980) and Phys. Rev. Letters 45, 867 (1980).

18) K. Fabricius, I. Schmitt, G. Schierholz and G. Kramer, DESY preprint DESY 80/91 (1980), to be published in Phys. Letters B.

19) A.V. Smilga and M.I. Vysotsky, Nucl. Phys. B150, 173 (1979).

20) G. Schierholz, Proc. of the SLAC Summer Institute on Particle Physics, Quantum Chromodynamics, July 9-20, 1979, ed. A. Mosher, p. 476;
P. Binétruy, Phys. Letters 91B, 245 (1980).

21) R.K. Ellis, D.R. Ross and A.E. Terrano, Caltech preprint CALT-68-785 (1980).

Figure Captions

Fig. 1 Tree diagrams for four-jet production.

Fig. 2 Four-jet event consisting of two back-to-back jets and definition of azimuthal angle ϕ . For oriented normals see text.

Fig. 3 Diagrams contributing to the leading qg and $\bar{q}g$ back-to-back jet configuration: (a) QCD and "QED", (b) QCD only.

Fig. 4 Phase space distribution of $\frac{d\sigma}{d\phi}$. Arbitrary units.

Fig. 5 Azimuthal distribution $\frac{1}{\sigma_0}\frac{d\sigma}{d\phi}$ for QCD and "QED".

Fig. 6 Azimuthal distribution $\frac{1}{\sigma_0}\frac{d\sigma}{d\phi}$ for oriented normals (see text) for QCD.

Fig. 7 Order α_s^2 three-jet diagrams (interfering with the tree diagrams). Self-energy diagrams which do only contribute to the real part are not shown here.

Fig. 8 The parameter P corresponding to γ-Z interference for $\sin^2\Theta_W = 0.23$.

Fig. 9 The asymmetry parameter R for $m_q/Q = 0.125$ and $m_q/Q = 0.25$ and various thrust values as a function of the angle between the quark and antiquark jet Θ_{12} .

Fig. 10 The Sterman-Weinberg cross section for three jets for $\epsilon,\delta = 0.2,\ 45^\circ$ and $\epsilon,\delta = 0.1,\ 30^\circ$ as a function of thrust. Also shown is the Born cross section.

Fig. 11 Thrust distribution $\frac{1}{\sigma}\frac{d\sigma}{dT}$ to order α_s^2 in the $\overline{MS}$ and TS scheme. Also shown is the Born cross section.

Fig. 12 The effective scale parameter Λ ($Q = 30$ GeV, $\Lambda_{\overline{MS}} = 0.3$ GeV, $N_f = 5$).

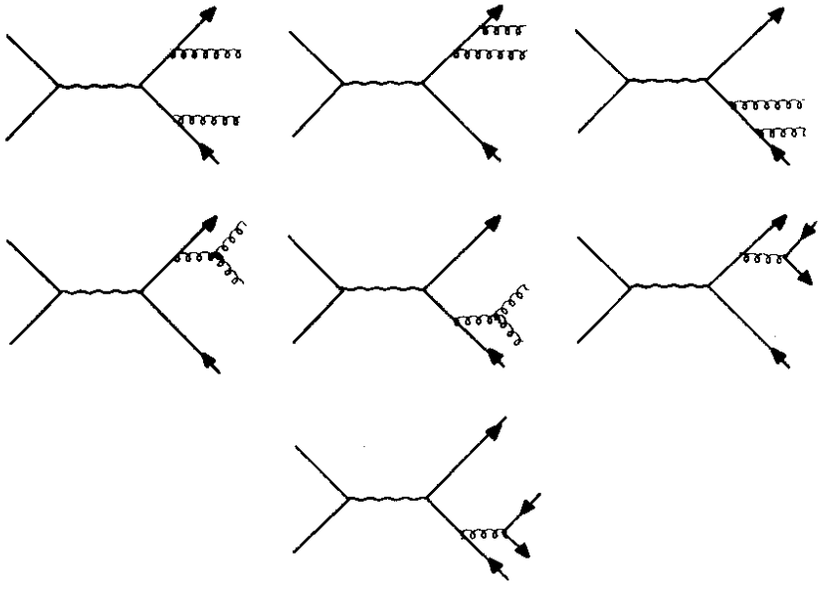

Fig. 1

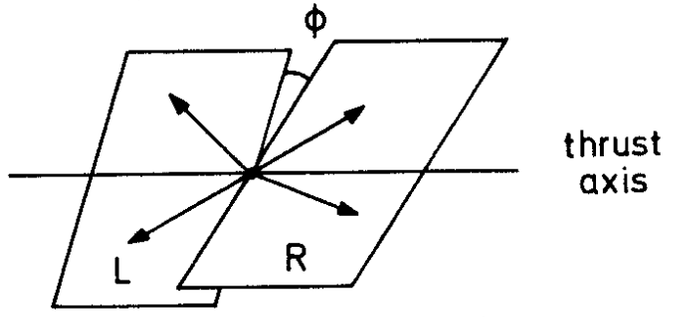

Fig. 2

(a) (b)

Fig. 3

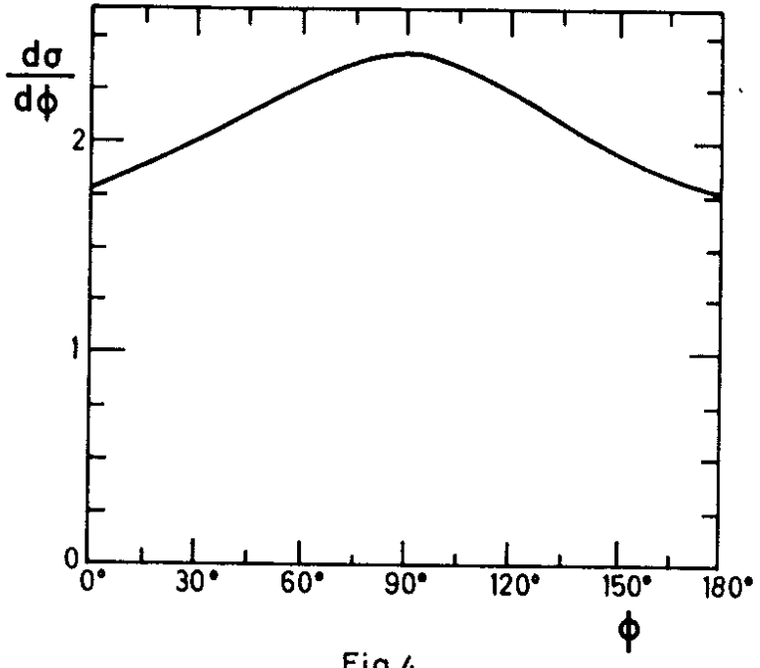

Fig. 4

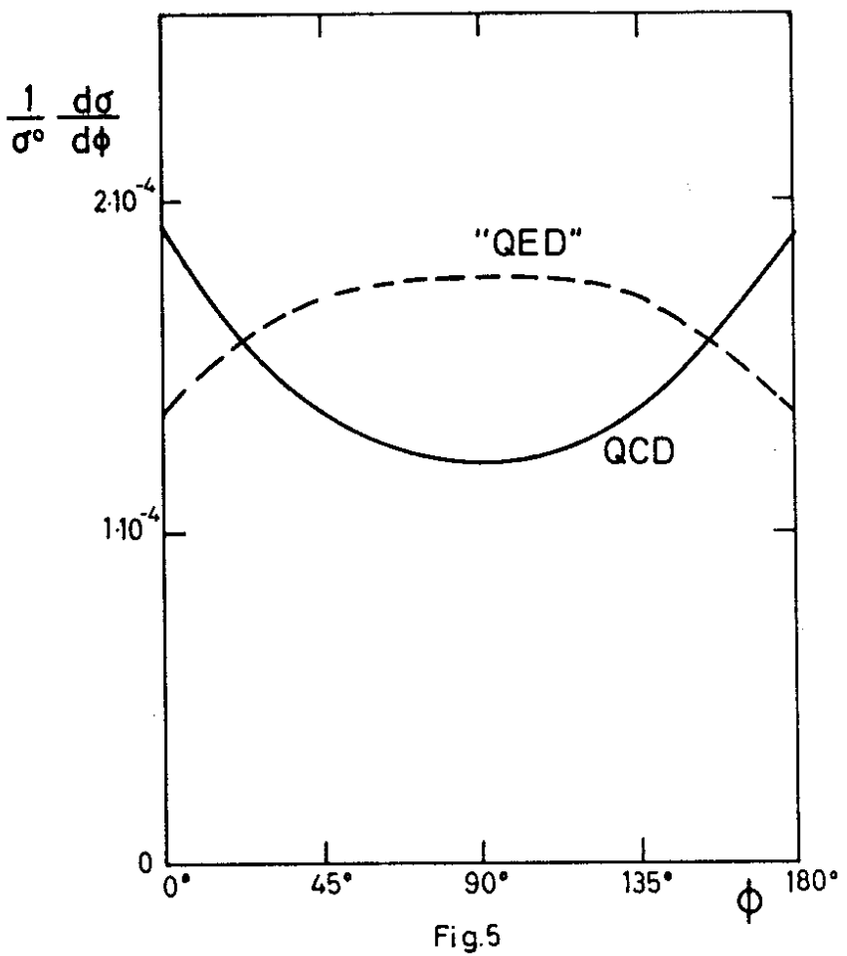
$\frac{1}{\sigma^\circ}\frac{d\sigma}{d\phi}$
$2\cdot10^{-4}$
$1\cdot10^{-4}$
0
"QED"
QCD
0°
45°
90°
135°
180°
ϕ

Fig.5

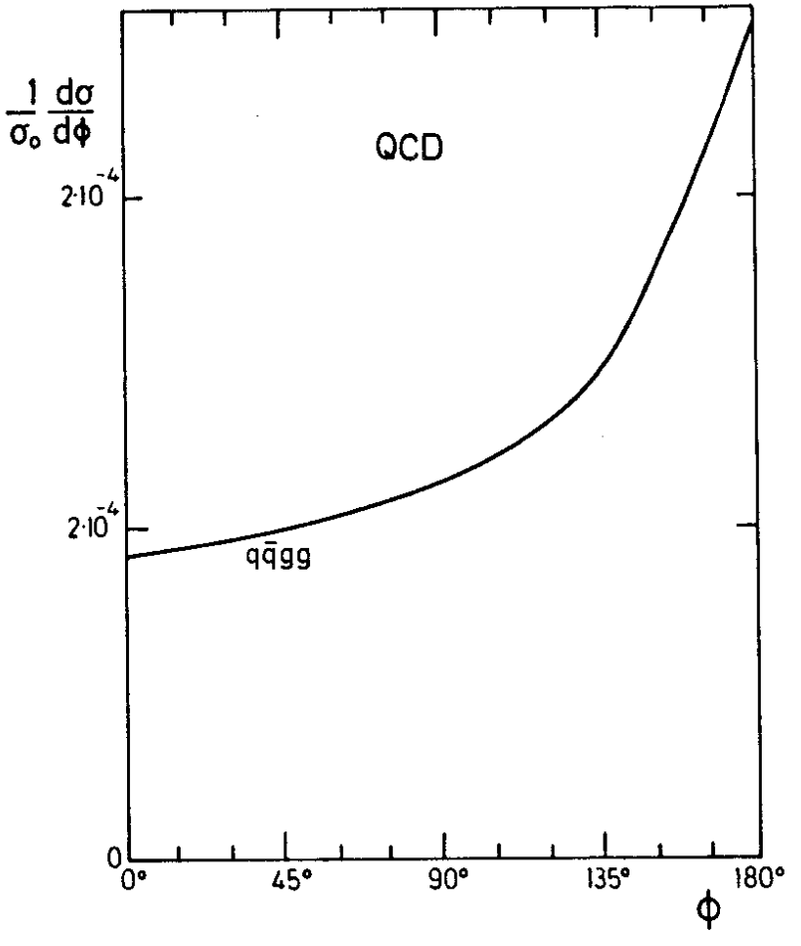
$\frac{1}{\sigma_o}\frac{d\sigma}{d\phi}$
QCD
$2\cdot10^{-4}$
$2\cdot10^{-4}$
0
$q\bar{q}gg$
0°
45°
90°
135°
180°
ϕ

Fig.6

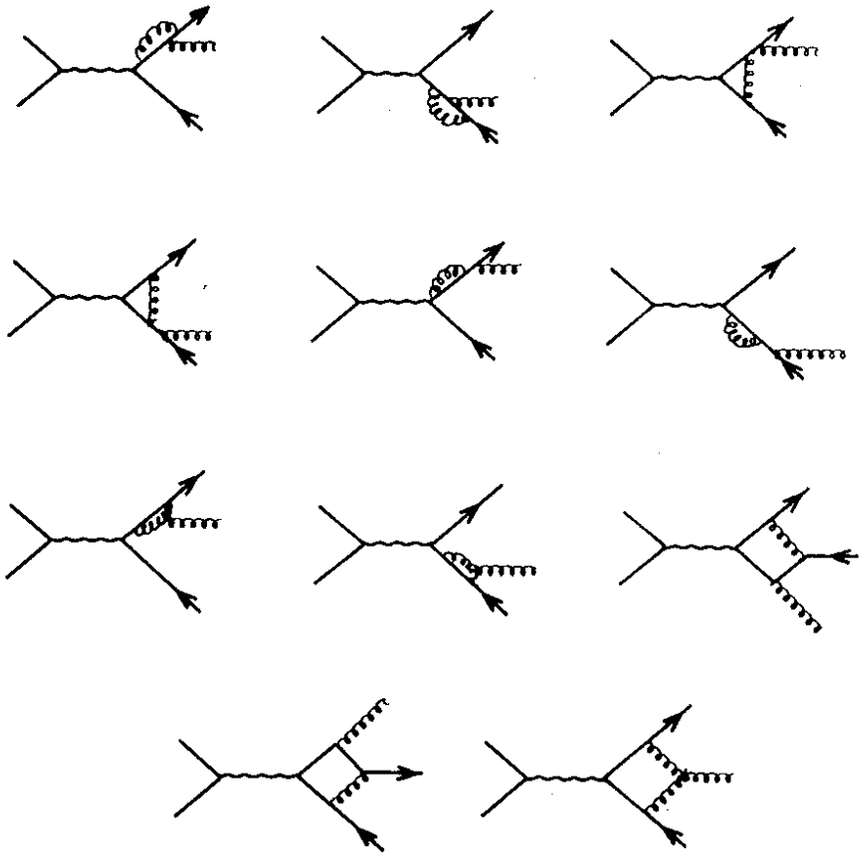

Fig.7

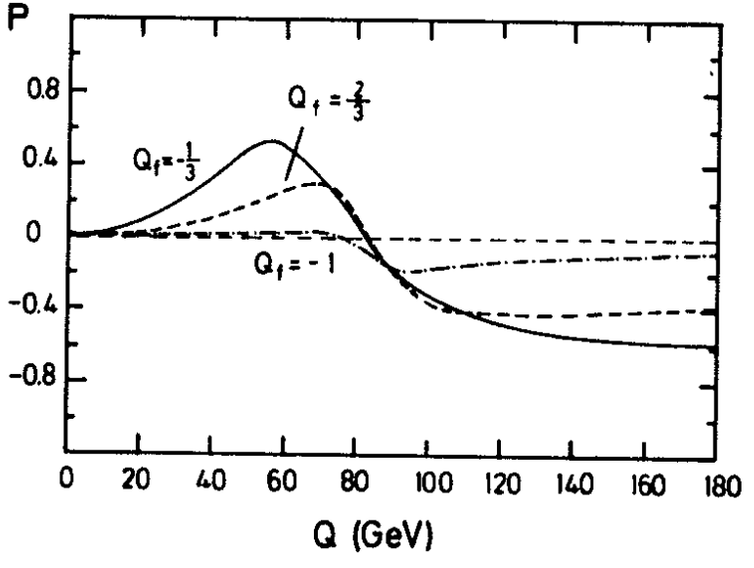
P
0.8
0.4
0
-0.4
-0.8
$Q_f = \frac{2}{3}$
$Q_f = -\frac{1}{3}$
$Q_f = -1$
0
20
40
60
80
100
120
140
160
180
Q (GeV)

Fig.8

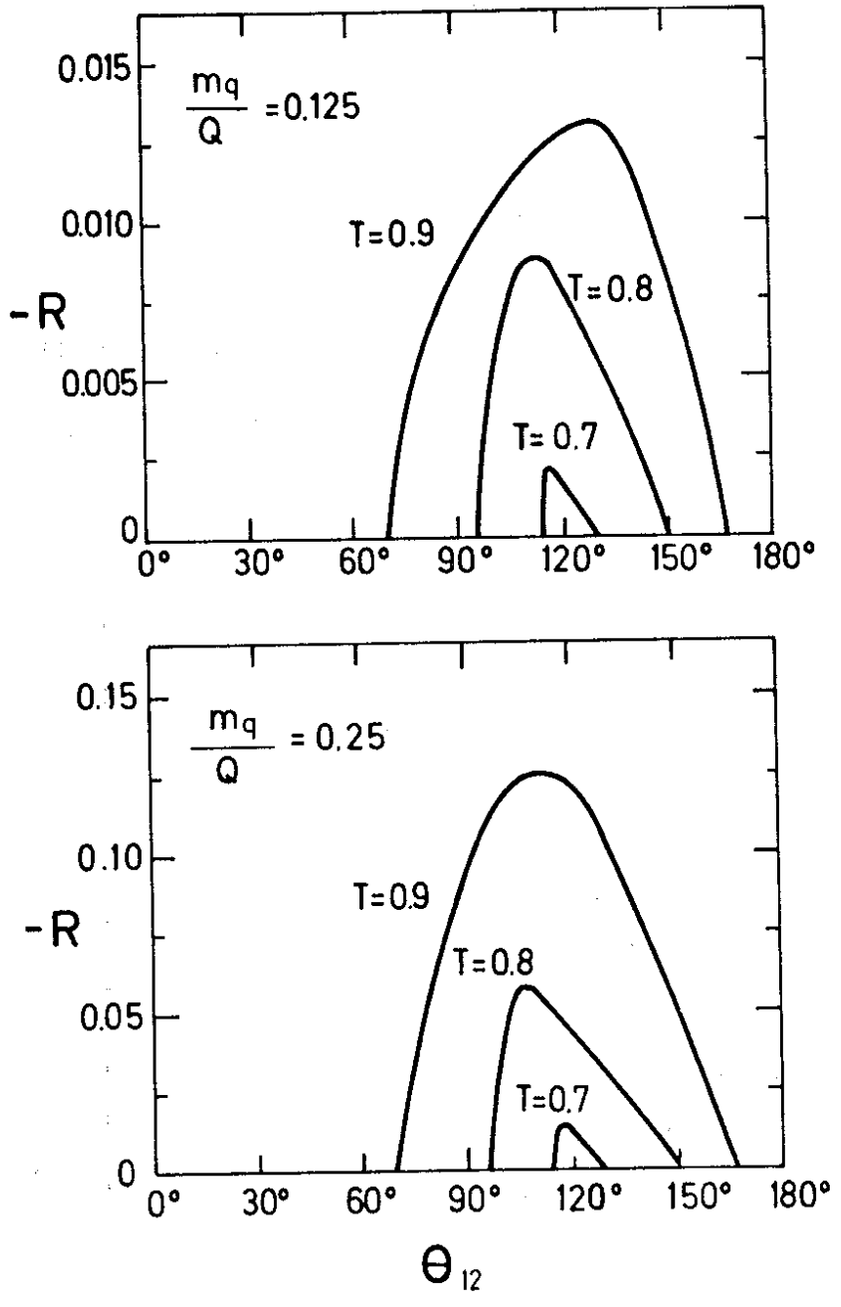
0.015
0.010
0.005
0
-R
mq/Q =0.125
T=0.9
T=0.8
T=0.7
0°
30°
60°
90°
120°
150°
180°
0.15
0.10
0.05
0
-R
mq/Q = 0.25
T=0.9
T=0.8
T=0.7
0°
30°
60°
90°
120°
150°
180°
θ12

Fig.9

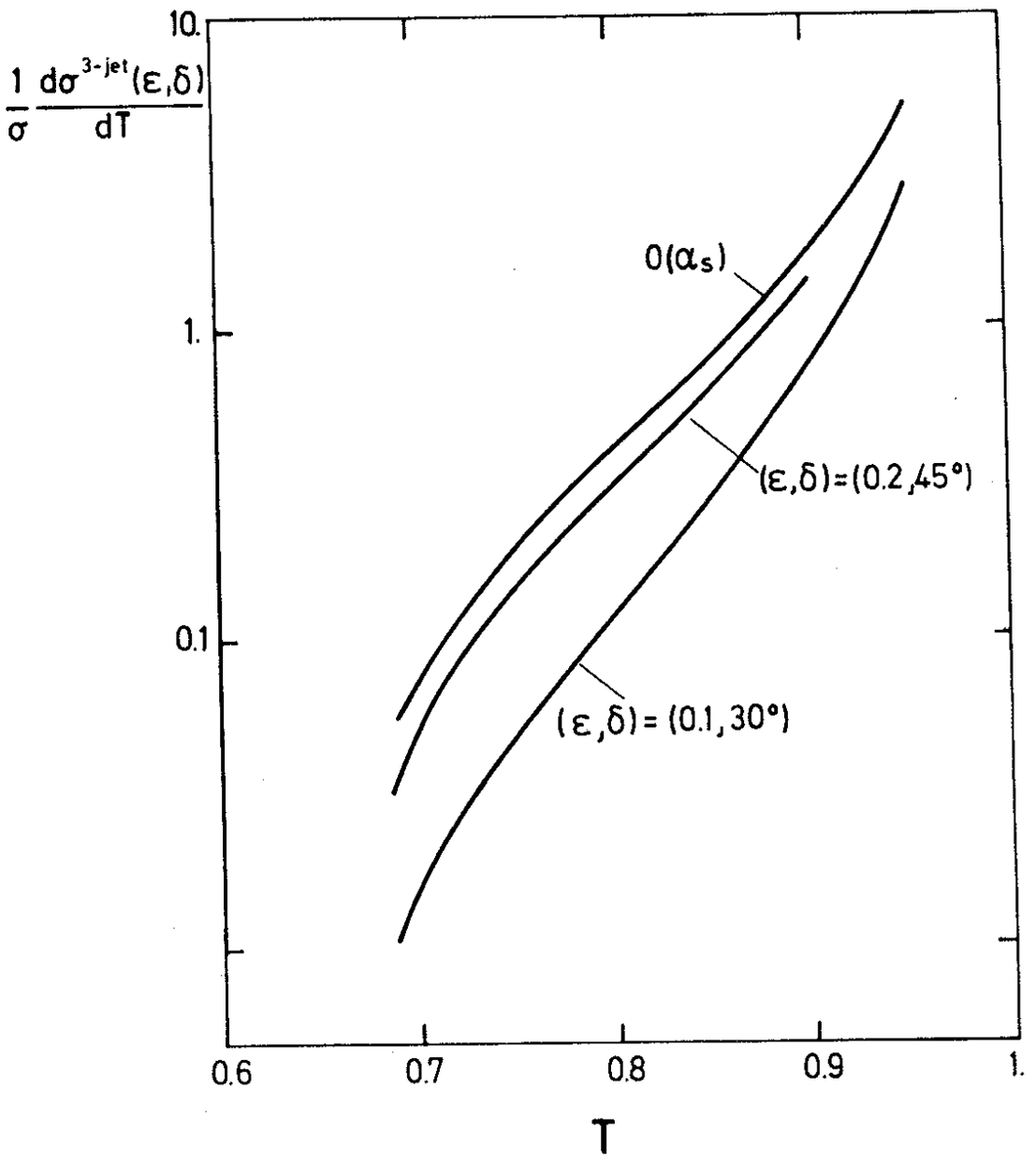
10.
1.
0.1
1/σ dσ3-jet(ε,δ)/dT
O(αs)
(ε,δ)=(0.2,45°)
(ε,δ)= (0.1,30°)
0.6
0.7
0.8
0.9
1.
T

Fig.10

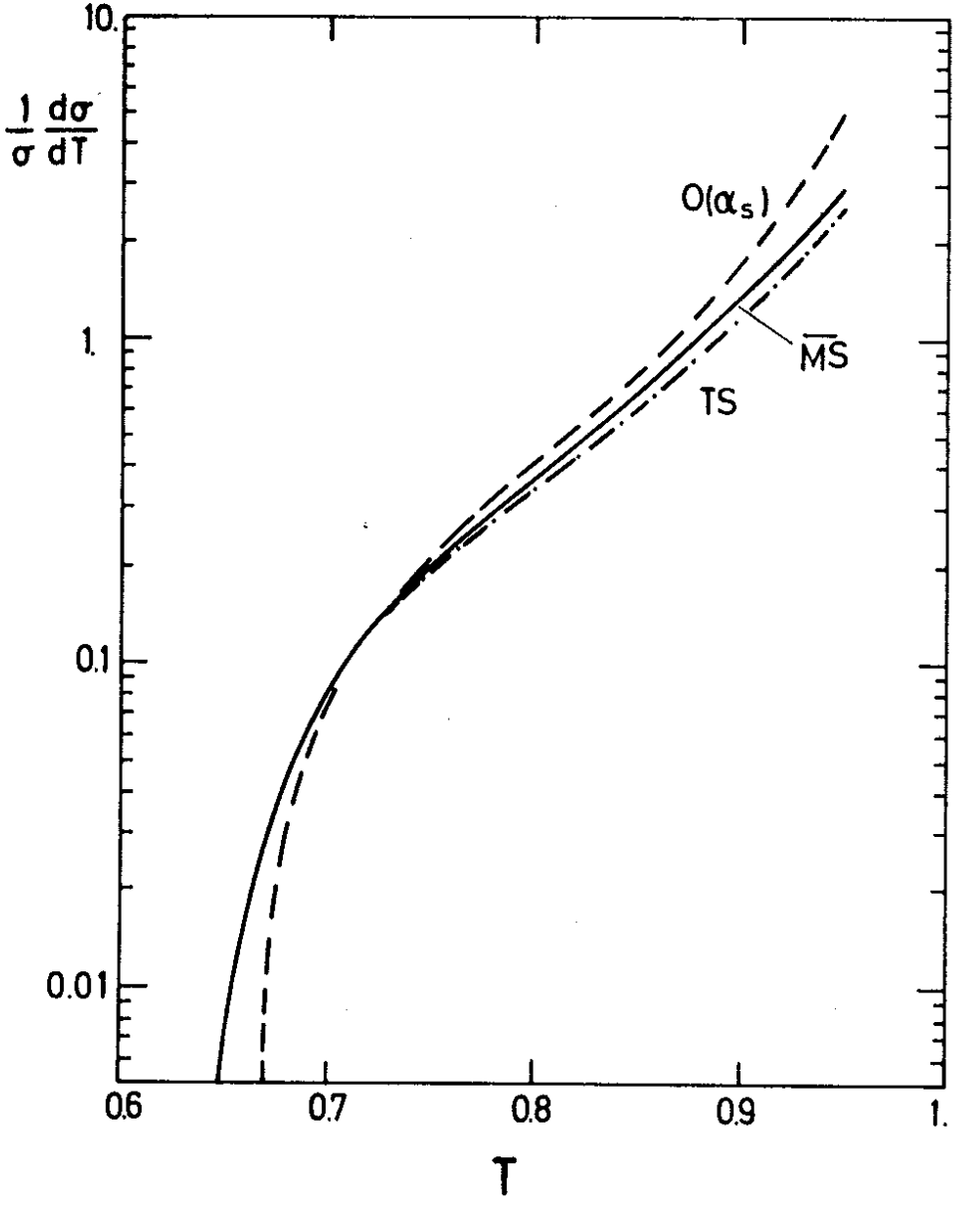
10.
1.
0.1
0.01
$\frac{1}{\sigma}\frac{d\sigma}{dT}$
$O(\alpha_s)$
$\overline{MS}$
TS
0.6
0.7
0.8
0.9
1.
T

Fig. 11

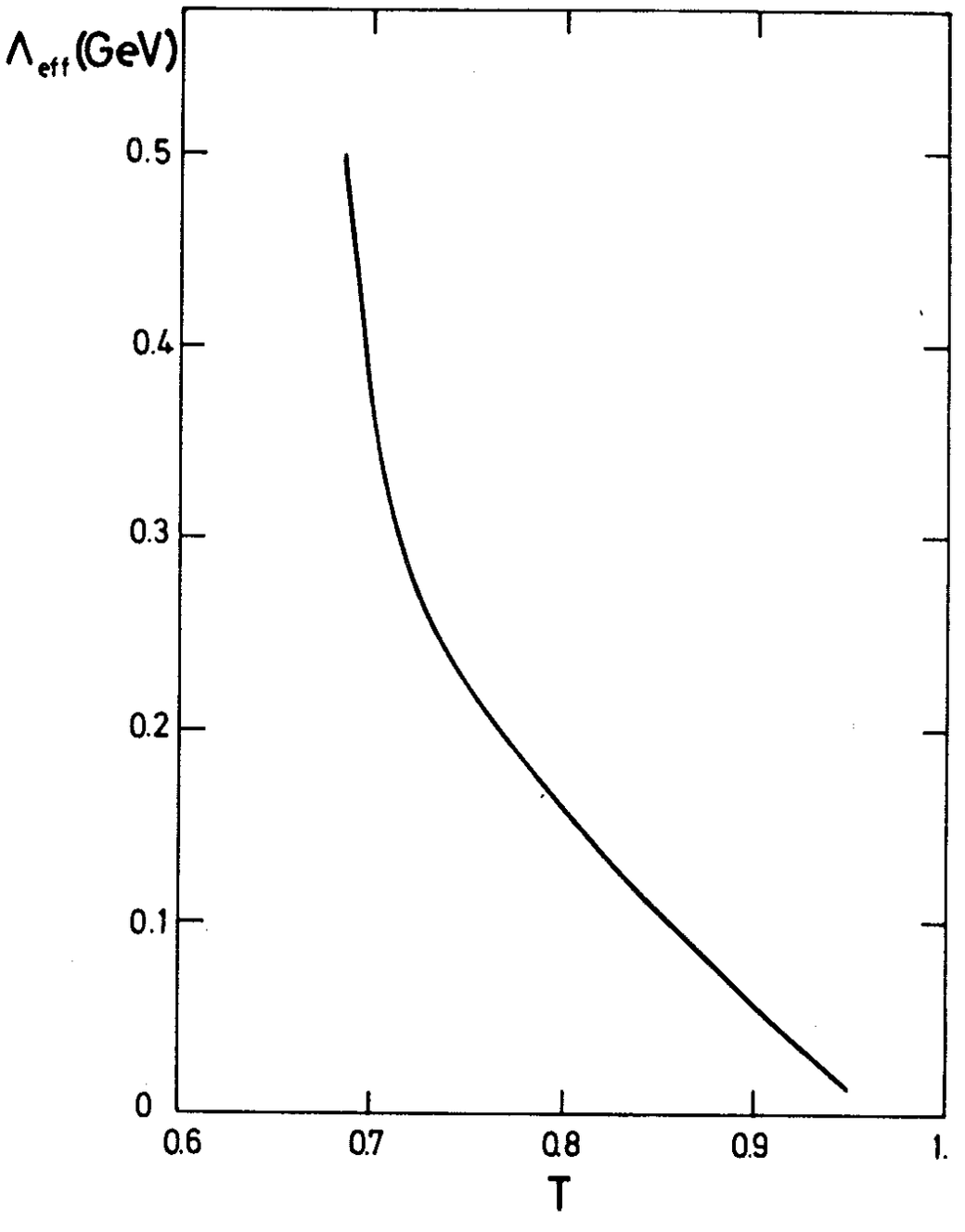
Λ_{eff}(GeV)
0.5
0.4
0.3
0.2
0.1
0
0.6
0.7
0.8
0.9
1.
T

Fig. 12